Supplemental Information

Anesthetic Binding in a Pentameric Ligand-gated Ion Channel: GLIC

Qiang Chen,[1♀] Mary Hongying Cheng,[2♀] Yan Xu,[1,3,4] Pei Tang[1,3,5*]

Departments of [1]Anesthesiology, [2]Chemistry, [3]Pharmacology and Chemical Biology, [4]Structural Biology, and [5]Computational Biology, University of Pittsburgh School of Medicine, Pittsburgh, PA 15260

[♀]These authors contributed equally to the work

I. Systems for MD simulations

The systems were setup using VMD package (1). The protonation states of titratable residues of GLIC at pH = 4.6 were estimated based on the pKa calculations by Bocquet et al (2). The distribution of deprotonated residues among five subunits was determined based on the calculation using Henderson-Hasselbalch equation. A binary POPE-POPG lipid mixture in a ratio of 3:1 was prepared to mimic the bacterial cell membrane. It was pre-equilibrated for 2 ns following an established procedure (3). The TM domain of GLIC was embedded in this equilibrated lipid patch and the rest part of GLIC was fully solvated by TIP3P water. The control system contained one protein, 263 POPE, 80 POPG, 82 Na^+, 11 Cl^- and 33,277 water molecules for a total of 168,430 atoms. Halothane systems were the same as the control except additional halothane molecules at different sites. Figure S1 shows two halothane systems that were used in MD simulations.

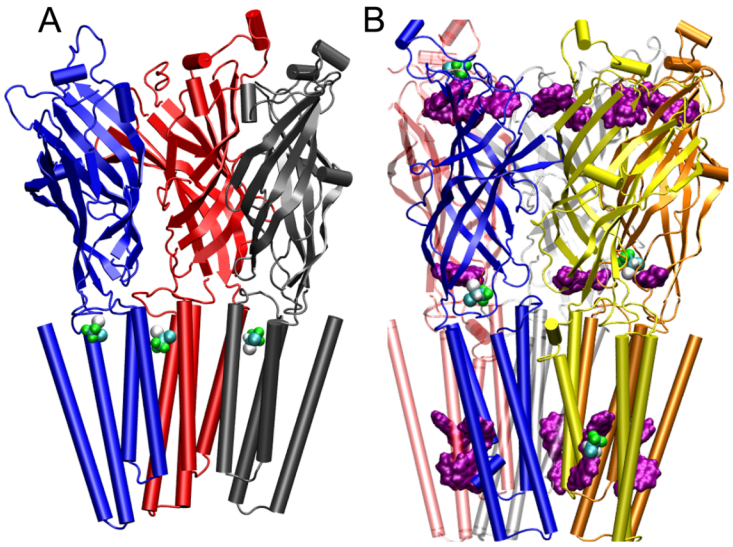

Figure S1: Halothane systems for MD simulations. For clarity, only halothane molecules and GLIC or part of GLIC are shown. (A) 3HAL-near-TM23 system, in which three halothane molecules were docked to the site near the TM23 loop. (B) 4HAL-near-TRPs system, in which four halothanes were docked to the Site-Trp^{EC} (near W47 and W72), Site-Trp^{INT} (near W160), and Site-Trp^{TM} (near W213 and W217). Trp residues are colored in purple. Individual subunits of GLIC were colored differently.

II. MD simulations

MD simulations were performed using the NAMD2 program (4). CHARMM27 force field with CMAP corrections (version 31) was used for protein, water, and lipids (5). The control system and the 3HAL-near-TM23 systems were energy minimized for 25,000 steps before 2-ns equilibration simulations, during which the constraint on the GLIC backbone was gradually reduced to zero. The 4HAL-near-TRP system was equilibrated for 1 ns after 10,000 steps of energy minimization. Finally, the unconstrained protein undergoes Nosé-Hoover constant pressure (P = 1 Bar) and temperature (T = 310 K) (6, 7) (NPT) simulation for more than 10 ns. In the MD simulations, we used periodic boundary conditions, water wrapping, hydrogen atoms constrained via SHAKE, and evaluated long-range electrostatic forces via the Particle Mesh Ewald (PME) algorithm (8). The bonded interactions and the short-range non-bonded interactions were calculated at every time-step (1 fs) and every two time-steps, respectively. Electrostatic interactions were calculated at every four time-steps. The cutoff distance for non-bonded interactions was 12 Å. A smoothing function was employed for the van der Waals interactions at a distance of 10 Å. The pair-list of the nonbonded interaction was calculated every 20 time-steps with a pair-list distance of 13.5Å.

III. Anesthetic docking in GLIC

Docking energy and occupancy for anesthetics at the sites studied by the fluorescence experiments are summarized in Table S1. For halothane (HAL), the docking results on both original crystal structure (termed as HAL_Xray) and MD-relaxed (termed as HAL_MD) structures are compared. For thiopental (THIO), only the results on the crystal structure are shown. The reported docking energy is the average from the energies of the docked anesthetics at a same site. The standard deviation is generally within 10%. Minor binding sites (other than experimental confirmed ones) are not listed in the Table S1. Docking occupancy represents the docking probability within 500 runs.

Table S1: Major anesthetic binding pockets in the GLIC

Binding pockets	***HAL_Xray***	***HAL_MD***	***THIO***
Site-Near-TM23-loop (Kcal/mol)	*-3.25*	*-3.04*	*-6.25*
Docking occupancy	*68%*	*15%*	*4%*
Site-Trp^{INT} (Kcal/mol)		*-3.42*	*-5.7*
Docking occupancy		*55%*	*31%*
Site-Trp^{EC} (Kcal/mol)		*-2.9*	*-5.20*
Docking occupancy		*5%*	*7%*
Site-Trp^{TM} (Kcal/mol)		*-2.89*	*-5.10*
Docking occupancy		*4%*	*13%*

IV. Supplemental Figures

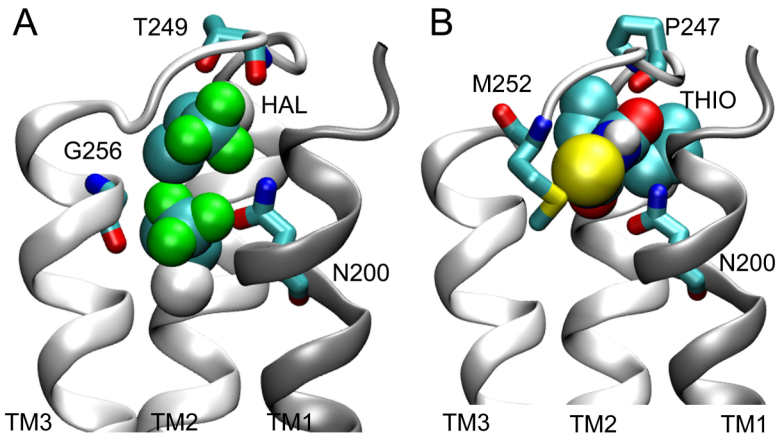

Figure S2: An inter-subunit binding pocket (termed as Site-near-TM23-loop), formed by N200 (TM1) from one subunit and the TM23 loop from the other subunit, was identified for (A) halothane and (B) thiopental by docking them on the crystal structure. Different subunits are colored in white and gray. Pocket lining residues are shown in licorice format. Anesthetics are shown in VDW format. Large yellow and white spheres represent sulfur and bromide atom in thiopental and halothane, respectively. Oxygen, nitrogen, carbon, hydrogen and fluorine atoms are shown in red, blue, cyan, white, and green respectively.

Figure S3: Alignment of a 5ns-MD-relaxed structure (yellow) with the crystal structure (green). There is no significant change between two structures.

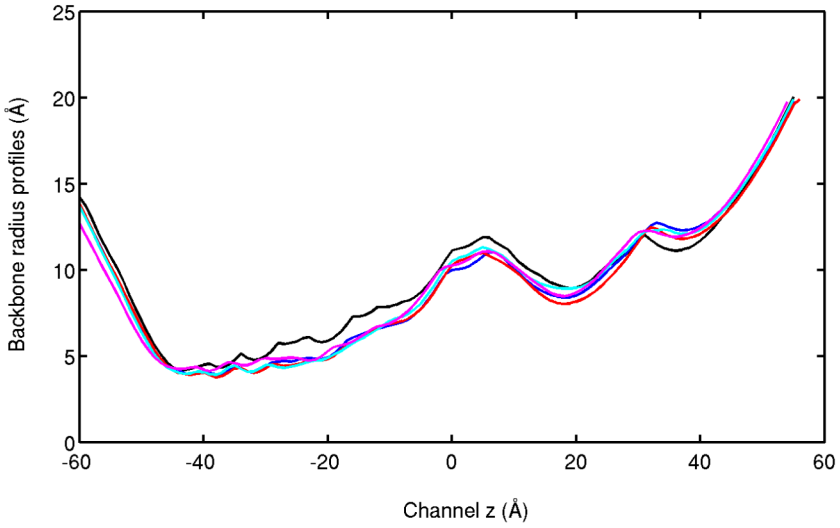

Figure S4: Comparison of the backbone pore radius profiles obtained from the crystal GLIC structure (black), the control system (blue), 3HAL-near-TM23 (cyan), and 4HAL-near-TRPs (red) systems. The pore radii were averaged over the last 100 frames near 10 ns MD.

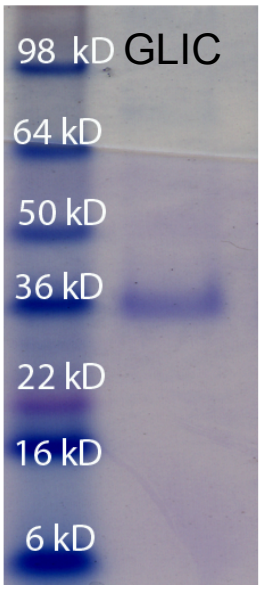

Figure S5: The SDS-PAGE of GLIC stained with Coomassie Blue. Stacking gel: 4% acrylamide/4% bisacrylamide in Laemmli stacking buffer. Resolving gel: 10% acrylamide/4% bisacrylamide in Laemmli resolving buffer. Running buffer: 3% Tris base, 14.4% glycine, and 0.75% SDS. The purity of GLIC is above 90%.

References

1. Humphrey, W., A. Dalke, and K. Schulten. 1996. VMD: visual molecular dynamics. *J. Mol. Graph.* 14:33-38.

2. Bocquet, N., H. Nury, M. Baaden, C. Le Poupon, J.-P. Changeux, M. Delarue, and P.-J. Corringer. 2009. X-ray structure of a pentameric ligand-gated ion channel in an apparently open conformation. *Nature* 457:111-114.
3. Chandler, D. E., J. Hsin, C. B. Harrison, J. Gumbart, and K. Schulten. 2008. Intrinsic curvature properties of photosynthetic proteins in chromatophores. *Biophys. J.* 95:2822-2836.
4. Phillips, J. C., R. Braun, W. Wang, J. Gumbart, E. Tajkhorshid, E. Villa, C. Chipot, R. D. Skeel, L. Kale, and K. Schulten. 2005. Scalable molecular dynamics with NAMD. *J. Comput. Chem.* 26:1781-1802.
5. MacKerell, A. D., Bashford, D., Bellott, M., Dunbrack, R.L., Evanseck, J. D., Field, M. J., Fischer, S., Gao, J., Guo, H., Ha, S., Joseph-McCarthy, D., Kuchnir, L., Kuczera, K., Lau, F.T.K., Mattos, C., Michnick, S., Ngo, T., Nguyen, D. T., Prodhom, B., Reiher, W.E., Roux, B., Schlenkrich, M., Smith, J. C., Stote, R., Straub, J., Watanabe, M., Wiorkiewicz-Kuczera, J., Yin, D., Karplus, M. 1998. All-atom empirical potential for molecular modeling and dynamics studies of proteins. *J. Phys. Chem. B* 102:3586–3616.
6. Nose, S. 1984. A unified formulation of the constant-temperature molecular-dynamics methods. *J. Chem. Phys.* 81:511-519.
7. Hoover, W. G. 1985. Canonical dynamics: Equilibrium phase-space distributions. *Phys. Rev. A* 31:1695-1697.
8. Darden, T., D. York, and L. Pedersen. 1993. Particle Mesh Ewald - an N.Log(N) Method for Ewald Sums in Large Systems. *J Chem Phys* 98:10089-10092.